Electrocatalytic Oxidation of 1,2-Cyclohexanediol to Adipic Acid with high Faradaic Efficiency under High Current Density Over a $CoFe_2O_4$@CuO/CF CatalystCatalyst

Xuzheng Cao[a], Gang Yan[a],* Qi Zhao[a], Huaqiao Tan[b],* Wensi Tang[b], Aicen Li[b], Yangguang Li[b],*

a College of Material Science and Engineering, Jilin Jianzhu University, Changchun 130118, China

b Key Laboratory of Polyoxometalate and Reticular Material Chemistry of Ministry of Education, Faculty of Chemistry, Northeast Normal University, Changchun, Jilin 130024, China,

Corresponding author: yang431@nenu.edu.cn; tanhq870@nenu.edu.cn (H.Q. Tan), liyg658@nenu.edu.cn (Y.G. Li)

Experimental section

Materials and chemicals

Cu foam (CF, thickness: 1 mm) was purchased from Suzhou keshenghe metal materials Co., Ltd. CF first was cleaned with diluted HCl, acetone, and deionized water for three times to remove surface oil and oxide layers. Then the cleaned CF is cut into a rectangle of 0.5×2 cm. Potassium hexacyanoferrate (III) $K_3[Fe(CN)_6]$, Cobalt sulfate ($CoSO_4 \cdot 7H_2O$), Sodium citrate ($Na_3C_6H_5O_7 \cdot 2H_2O$), Ammonium persulfate ($(NH_4)_2S_2O_8$, AR), Sodium hydroxide (NaOH, AR) and Potassium hydroxide (KOH) were purchased from Shanghai Aladdin Bio-Chem Technology Co., LtD.

Synthesis of CuO nanostructures on CF.

Typically, a piece of treated CF (0.5×2 cm) is immersed into the solution at room temperature (2.5 M NaOH and 0.13 M $(NH_4)_2S_2O_8$). After 30 min, the CF was rinsed with ethanol and deionized water, and then dried. The CF was calcined in air at 300 ℃ for 3 h to convert the $Cu(OH)_2$ to CuO.

Synthesis of $KCo[Fe(CN)_6]$@CuO/CF nanocube arrays

The template-directed growth of well-aligned Prussian-blue-analog (PBAs) nanocubes arrays of $KCo[Fe(CN)_6]$ on the surface of $Cu(OH)_2$ nanowires were prepared using a facile method. In the synthesis, 5.294 g (18 mmol) trisodium citrate dihydrate ($Na_3C_6H_5O_7 \cdot 2H_2O$) and 1.498 g (6 mmol) Cobalt sulfate [$CoSO_4 \cdot 7H_2O$] were dissolved in 200 mL of distilled water to form solution A. 1.316g (4 mmol) potassium hexacyanoferrate (III) $KCo[Fe(CN)_6]$ was dissolved in 200 mL of distilled water to form solution B. Then, solution B was slowly added into solution A at room temperature under an ambient atmosphere. After the mixture was stirred for 15 min, the CuO nanosheets grown on Cu foam were immersed in the solution and the solution was sealed and heated at 40 °C for 1 h. Then, the obtained solution was cooled down to room temperature and aged for 10 h at room temperature. As the reaction goes on, the obtained $KCo[Fe(CN)_6]$@CuO nanocube arrays grown on CF were collected and washed with doubly distilled water and ethanol, and then dried under vacuum at 60 °C for 12 h.

Synthesis of $CoFe_2O_4$@CuO/CF

The obtained precursor $KCo[Fe(CN)_6]$@CuO/CF were placed at in the tube furnace. Subsequently, the sample was heated to 300 °C at a heating rate of 5 °C min^{-1} for 3 h, $CoFe_2O_4$@CuO/CF nanocubes was obtained.

Characterizations

The crystallinity and crystalline phases composition of the samples were tested by Powder X-ray diffraction (PXRD) on Smart lab X-ray diffractometer instrument with Cu-Kα radiation source (λ = 1.54056 Å). The accelerating voltage of 30 kV and emission current of 30 mA were used. Energy Dispersive X-ray (EDX) analysis and the surface morphology of samples were acquired by JEOL JSM 4800F scanning electron microscope. Transmission electron microscopy (TEM), High-resolution images (HRTEM) and element maps were studied on a JEOL-2100F microscope with a 200 kV acceleration voltage. To study the valance band state and chemical state of the photocatalysts, we received the X-ray photoelectron spectroscopy (XPS) results of the catalyst samples with the PHI Quantum ESCA microprobe system, using the Mg K_α line of a 250-W Mg X-ray tube as a radiation source with the energy of 1253.6 eV,

16 mA × 12.5 kV and the working pressure of lower than 1×10^{-8} Nm^{-2}. As an internal reference for the absolute binding energy, the C 1s peak at 284.80 eV of hydrocarbon contamination was used. After CHD electro-oxidation reaction, high performance liquid chromatography (HPLC) was performed with a refractive index detector (RID) and a UV-Vis detector (UVD) to analyze selectivity and Faradaic efficiency of products. an organic acid column (7.8 mm × 300 mm, 10 μm) was used with column temperature of 55 °C and RID temperature of 40 °C for the HPLC. 0.01M H_2SO_4 eluent with flow rate of 0.5 mL/min was used. The product concentration was determined by the calibration curves of standard solutions with given concentrations in order to conduct the quantitative analysis of reaction substrates and corresponding oxidation products. The liquid before and after the CHD oxidation reaction was analyzed using HPLC to determine the CHD conversion, selectivity of product and yield of product. Various products during the electrocatalytic conversion of CHD to AA were tested by the liquid chromatography–mass spectrometer (LC–MS) on an Agilent 6550 QTOF instrument. A C18 column and a UV detector (λ = 227 nm) were employed, and acetonitrile/water (60/40, v/v) was used as the mobile phase at a flow rate of 1.0 mL/min.

Electrochemical measurements

CHI 660E electrochemical workstation (Shanghai Chenhua, China) was used to test the electrochemical performance of catalysts in a typical three-electrode system. The electrolyte was 1 M KOH (pH=14). Co_2O_4@CuO/CF works directly as a working electrode. Carbon rod and calomel electrode as the counter electrode and the reference electrode, respectively. The working surface area of the electrode maintained 1 cm^2 , with the rest of the electrode sealed with a modified acrylate adhesive. Carbon rod electrode and the working electrode surface area (1 cm^2) is the same as those of $CoFe_2O_4$@CuO/CF. The tested potentials vs. Hg/HgO are converted to the reversible hydrogen electrode (RHE) based on Evs.E(RHE) = E(Hg/HgO) + 0.05916 × pH + 0.1989. The linear sweep voltammetry (LSV) curves were obtained at the scan rate of 0.1 mV s^{-1}. The i-t curves were tested to study the stability of catalysts. The polarization curves data have been made with iR compensation.

Estimation of effective electrode surface area

The ECSA (electrochemical surface area) was evaluated with cyclic voltammograms (CV) measurement at non-faradaic overpotentials. The CV measurements were performed at various scan rates (10, 20, 30, 40, and 50 mV/s) in 0.1-0.3 V vs. RHE. A linear trend was observed by plotting the difference of current density between the anodic and cathodic at 0.2 V vs. RHE against the scan rate. The double layercapacitance (C_{dl}) is equal to half of the slope of the fitting line. The slope is proportional to the electrode surface area of catalysts. Therefore, the electrochemical surface areas of different samples can be compared based on their C_{dl} values.

Measurements of electrochemical impedance spectroscopy (EIS)

The operated overpotential was 0.2 V vs. RHE. The electrochemical impedance spectroscopy (EIS) was conducted from at certain potential with frequency from 0.01 Hz to 100000 Hz. A sinusoidal voltage with an amplitude of 5 mV were appliedtocarry out the measurements.

The apparent activation energy

The apparent electrochemicalactivation energy (E_{app}) for CHD oxidation can be determined using the Arrheniusrelationship: $d(\log i_k)/d(1/T) = E_{app}/2.3R$, where i_k is the kinetic current at a potential of 1.5 Vvs. RHE, T is the temperature, and R is the universal gas constant (8.314 J $mol^{-1}\cdot K^{-1}$). Fromthe slop of the Arrhenius plots at a potential of 1.5 V vs. RHE, the apparent electrochemicalactivation energy can be extracted.

Measurements of Bode plots

Bode plots testswere measured using a CHI 660E electrochemical workstation over a frequency range from 10^4 to 10^{-1} Hz with an amplitude of 10 mV in 1 M KOH with/without 0.1 M CHD and AC amplitude of 5 mV potential.

Measurements of In-situ Raman

In-situ Raman spectroscopy was obtained on a laser confocal Raman spectrometer (LabRAM HR) equipped with an objective of 50X LWD using a 532 nm laser as the excitation source at controlled potentials by a CHI 660E electrochemical workstation. The in-situ electrolytic cell was assembled by Teflon with a piece of round quartz glass

as the cover. The $CoFe_2O_4$@CuO/CF electrode was set to keep the plane of the electrode perpendicular to the incident laser. A graphite rod and Hg/HgO electrode were used as the counter electrode and reference electrode, respectively. The Raman spectra were collected under chronoamperometry (I-t) at different potentials in 1.0 M KOH containing 0.1 M CHD as the electrolyte.

Measurements of Open-circuit potential (OCP)

The open-circuit potential (OCP) is the potential at which the current of the test system approaches zero, reflecting changes in adsorbed species on the catalyst surface. Under open-circuit potential (OCP) conditions, the voltage was recorded after the voltage change was less than 1 mV in 100 s. Then, 0.1 M CHD was added, and then the voltage was recorded after waiting for the voltage to stabilize, and the difference between the two recorded voltages was the OCP value.

Assembly and testing of the two-electrode system

The two-electrode electrochemical test system was carried out in an H-shaped electrolytic cell. The overall electrolysis used Pt||$CoFe_2O_4$@CuO/CF as anode and cathode, with an anionic membrane separating the electrolyte of 1 M KOH with 0.1 M CHD in anodic chamber and the electrolyte of 1.0 M KOH solution in cathodic chamber. An anionic membrane was pretreated in 0.5-1.0 M KOH solution at 20 ℃-30 ℃ for 24 h, then washed with deionized water. The membrane need to be stored in 0.5-1.5 wt% NaCl solution for short to medium term storage. The LSV curve was tested on an electrochemical workstation with a voltage range of 0 V to 2.5 V. And the LSV curve was measured at a scan rate of 10 mV s^{-1}.

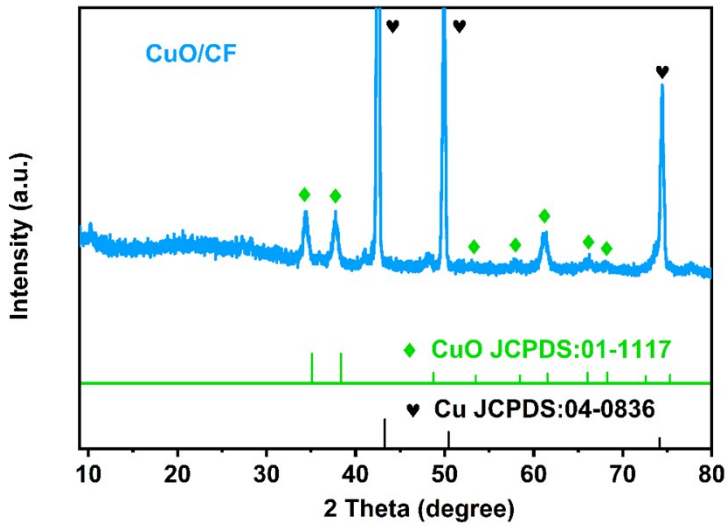

Fig. S1. XRD pattern of CuO/CF

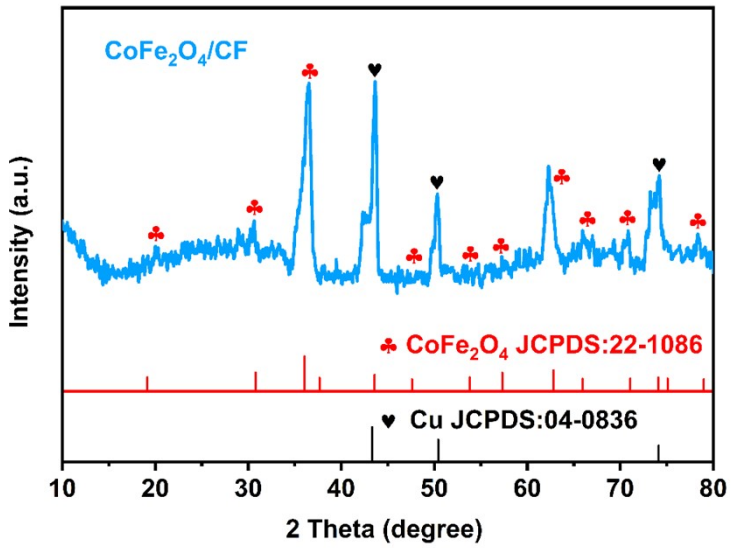

Fig. S2. XRD pattern of $CoFe_2O_4$ /CF

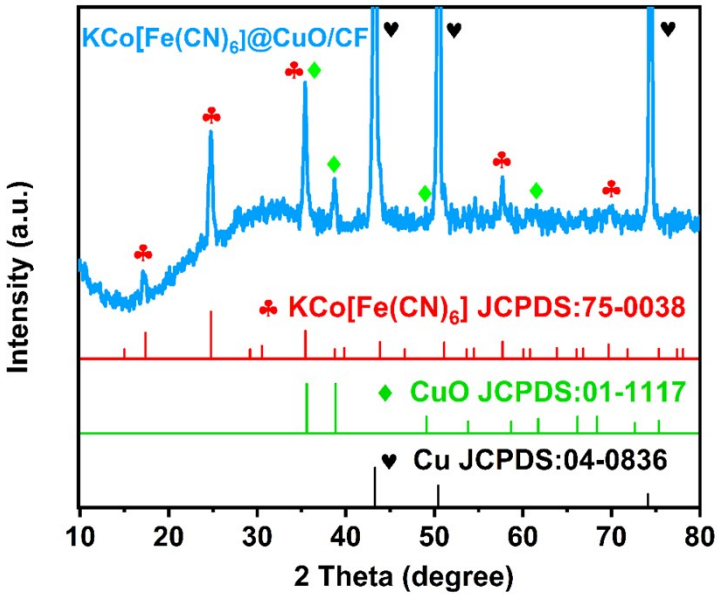

Fig. S3. XRD pattern of $KCo[Fe(CN)_6]$@CuO/CF

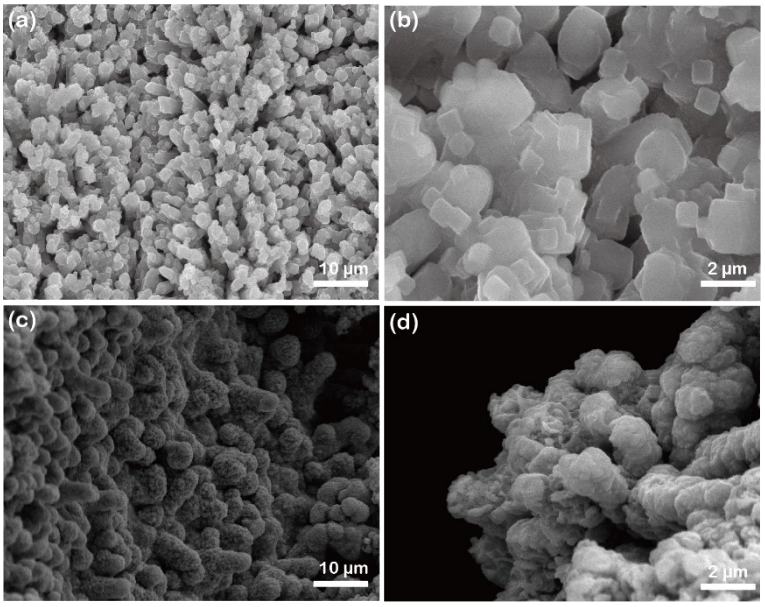

Fig. S4. SEM image of (a, b) $KCo[Fe(CN)_6]$@CuO/CF, (c, d) $CoFe_2O_4$/CF

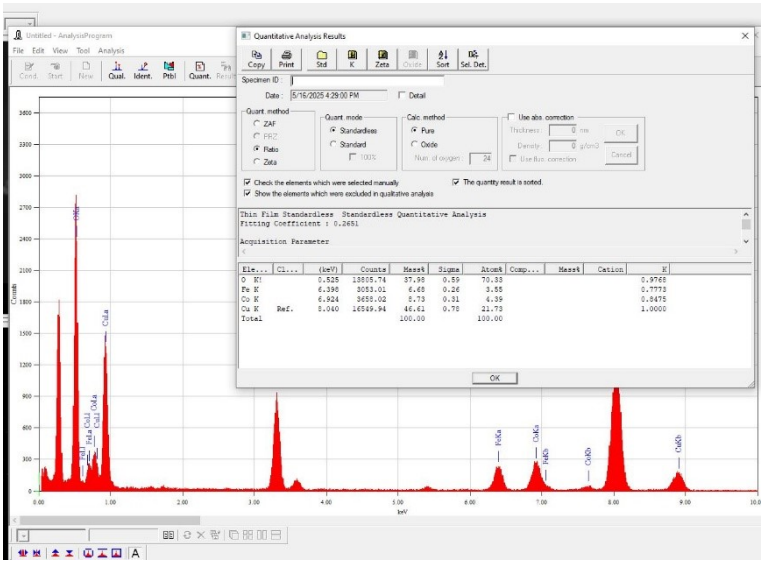

Fig. S5. EDX analysis of the $CoFe_2O_4$@CuO/CF.

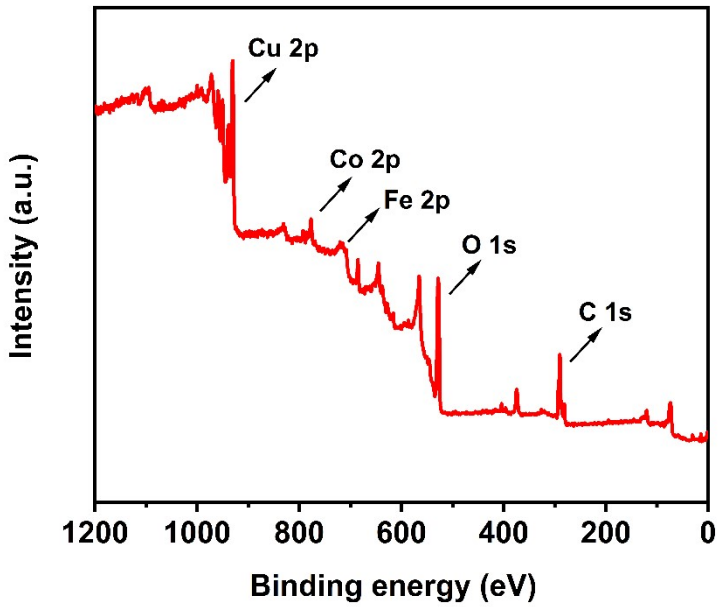

Fig. S6. Full XPS spectrum of $CoFe_2O_4$@CuO/CF.

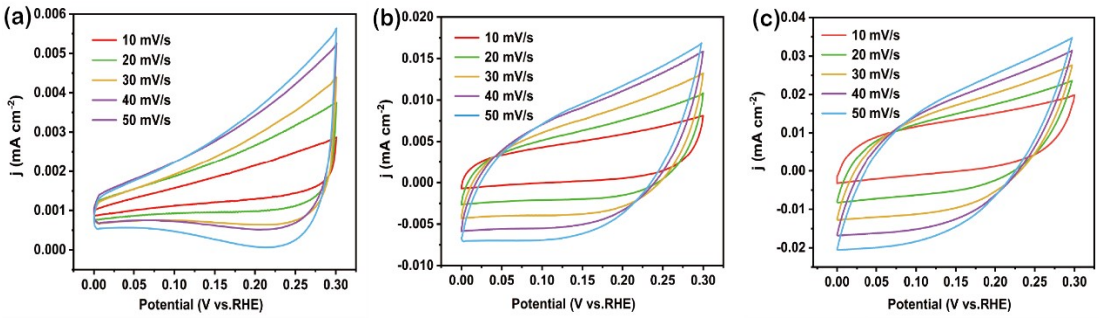

Fig. S7. Cyclic voltammograms (CVs) of (a) CuO/CF, (b) $CoFe_2O_4$ /CF, (c) $CoFe_2O_4$@CuO/CF.

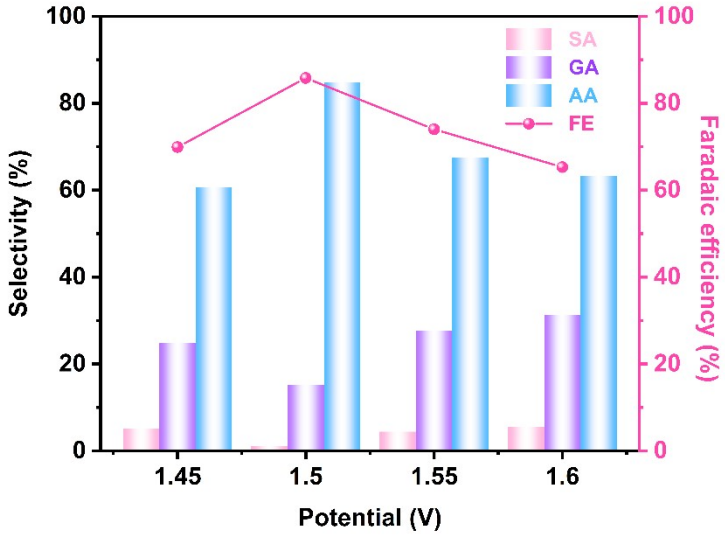

Fig. S8. The products selectivity and the Faradaic efficiency after the CHD oxidation at different applied potentials using $CoFe_2O_4$@CuO/CF as electrocatalyst.

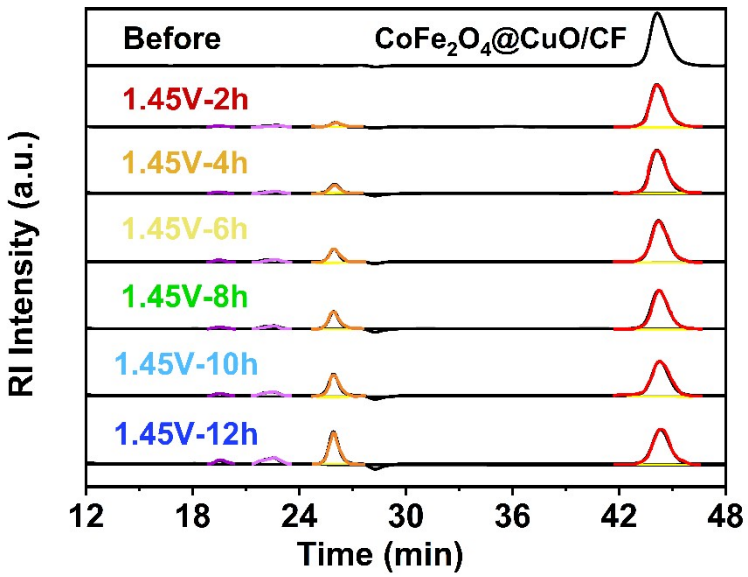

Fig. S9. HPLC chromatograms of the reaction products from the electrochemical oxidation of CHD using $CoFe_2O_4$@CuO/CF as electrocatalyst at 1.45V.

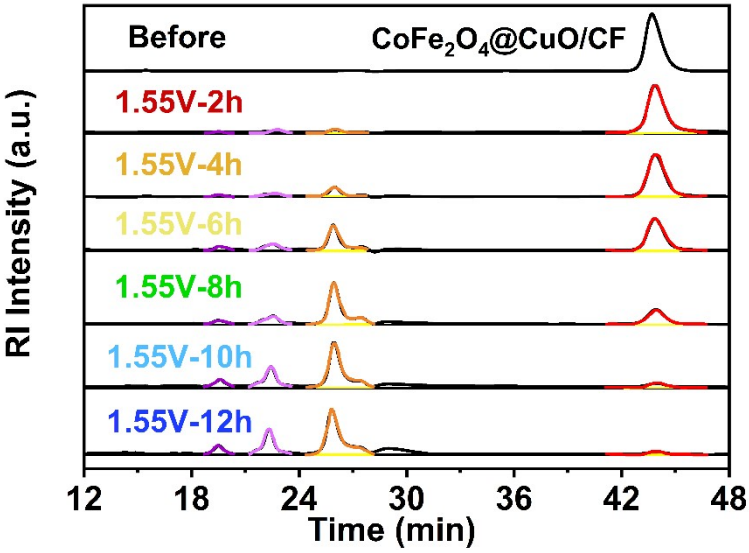

Fig. S10. HPLC chromatograms of the reaction products from the electrochemical oxidation of CHD using $CoFe_2O_4$@CuO/CF as electrocatalyst at 1.55V.

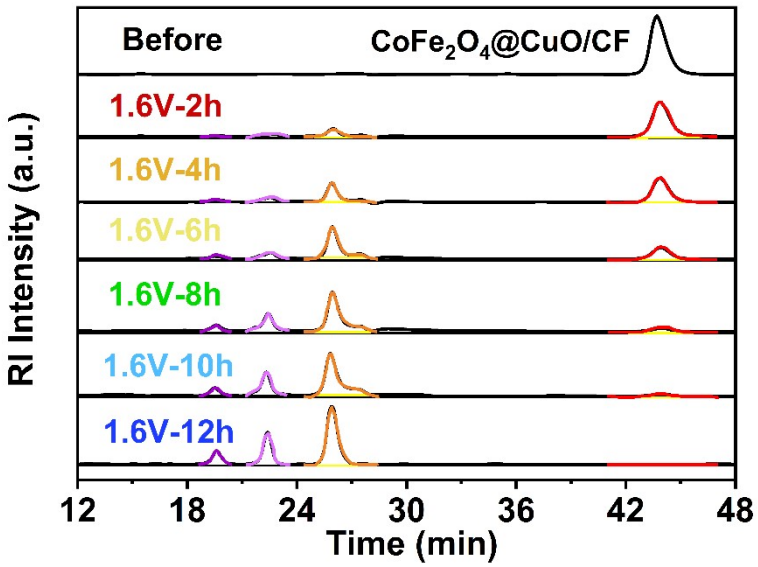

Fig. S11. HPLC chromatograms of the reaction products from the electrochemical oxidation of CHD using $CoFe_2O_4$@CuO/CF as electrocatalyst at 1.6V.

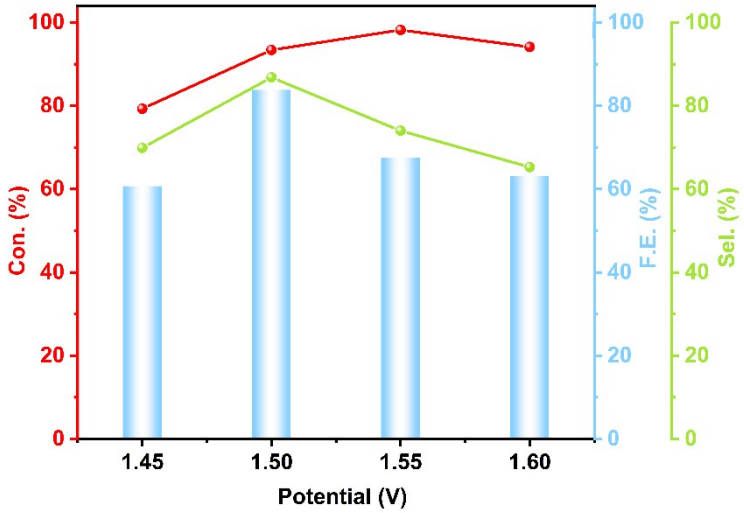

Fig. S12. The conversion rate, FE, and selectivity of different voltages using $CoFe_2O_4$@CuO/CF as electrocatalyst.

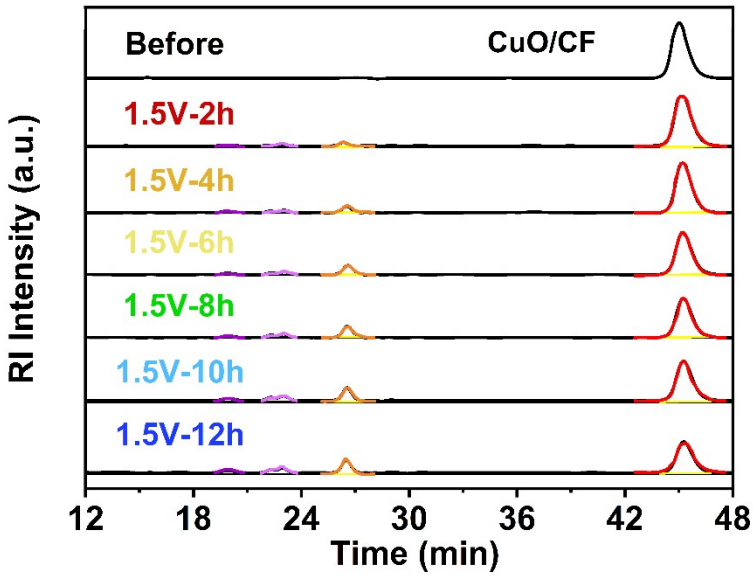

Fig. S13. HPLC chromatograms of the reaction products from the electrochemical oxidation of CHD using CuO/CF as electrocatalyst at 1.5V.

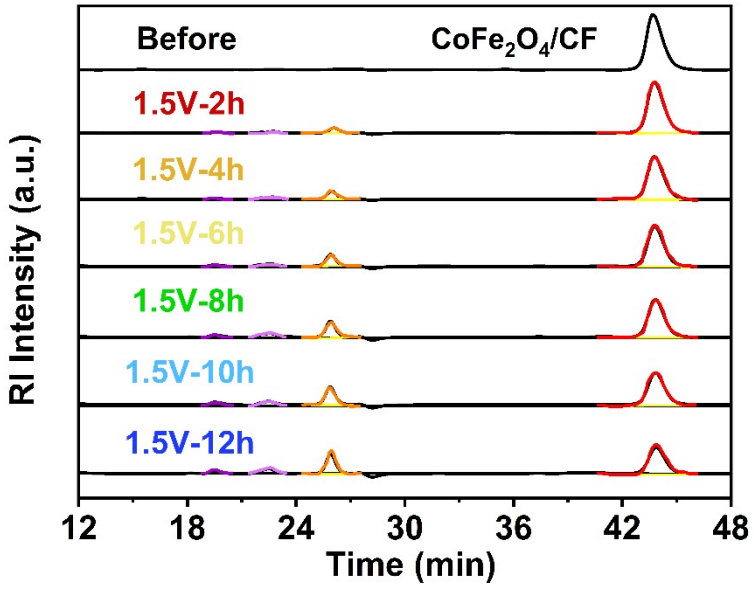

Fig. S14. HPLC chromatograms of the reaction products from the electrochemical oxidation of CHD using $CoFe_2O_4$/CF as electrocatalyst at 1.5V.

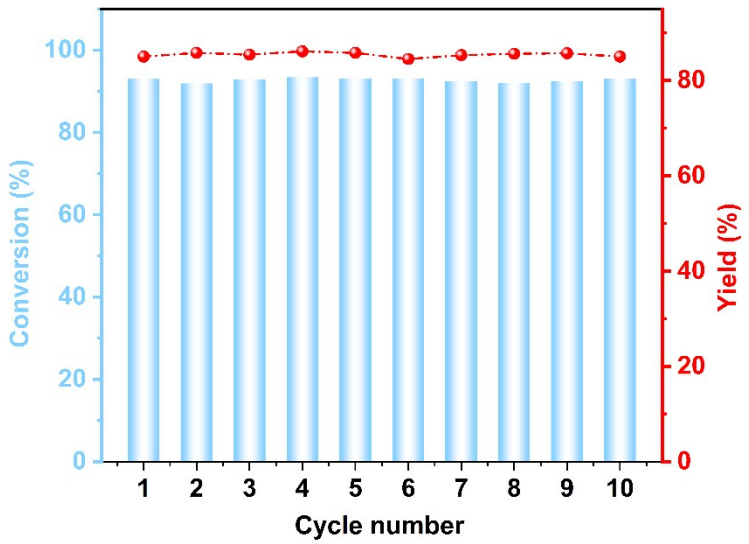

Fig. S15. The conversion rate, and yield of different cycles using $CoFe_2O_4$@CuO/CF as electrocatalyst.

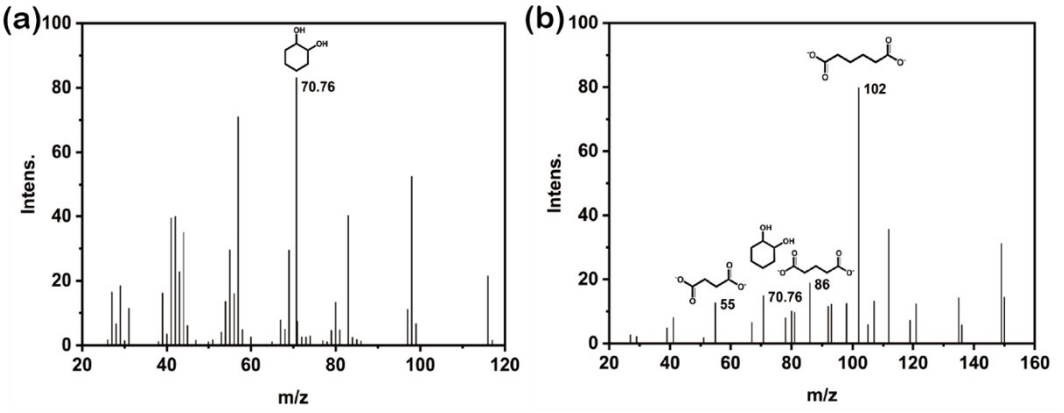

Fig. S16. (a) LC-MS results before electrocatalytic CHD, (b) Chromatogram of LC-MS monitoring after electrocatalytic CHD.

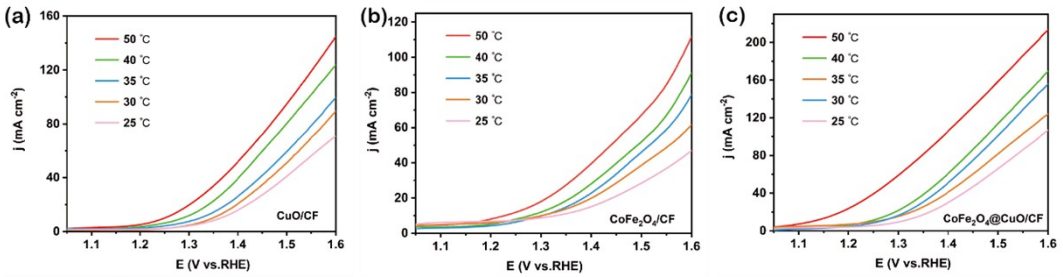

Fig. S17. The compared performances in 1.0 M KOH with 0.1 M CHD at 25 °C,30 °C, 35 °C, 40 °C, 50 °C. (a) CuO/CF, (b) $CoFe_2O_4$/CF and (c) $CoFe_2O_4$@CuO/CF.

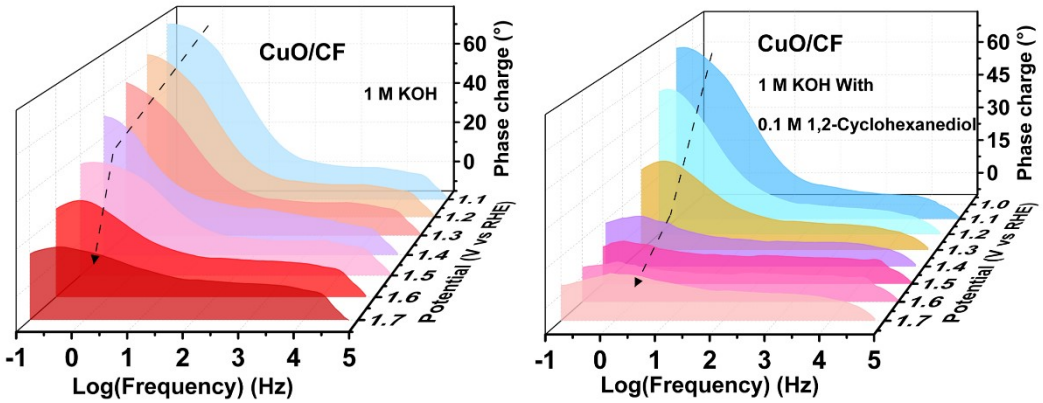

Fig. S18. Bode plots of CuO/CF in 1.0 M KOH (a) with and (b) without 0.1 M CHD

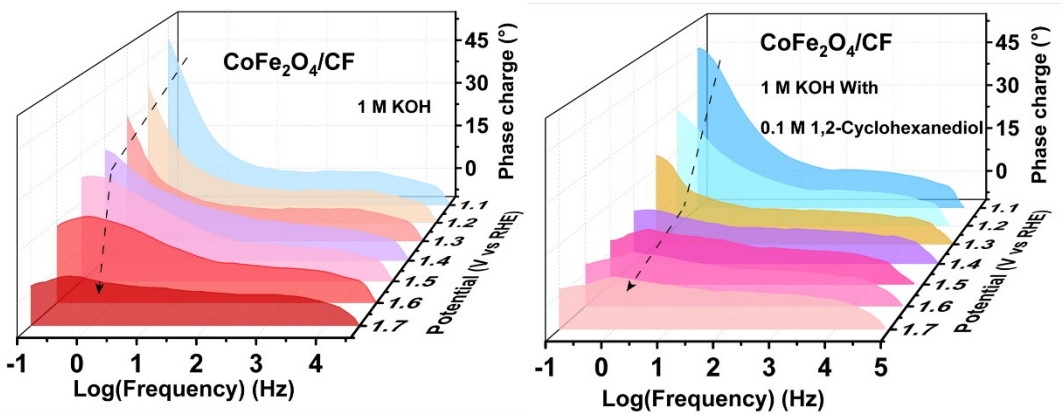

Fig. S19. Bode plots of $CoFe_2O_4$/CF in 1.0 M KOH (a) with and (b) without 0.1 M CHD

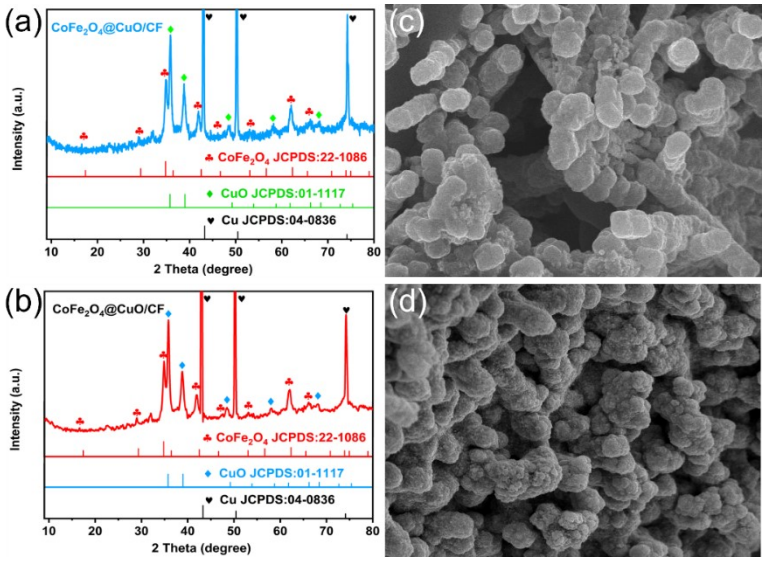

Fig. S20. The XRD images of catalyst (a) before and (b) after 50 h electrolysis at 300 mA cm^{-2}. The SEM images of catalyst (c) before and (d) after 50 h electrolysis at 300 mA cm^{-2}

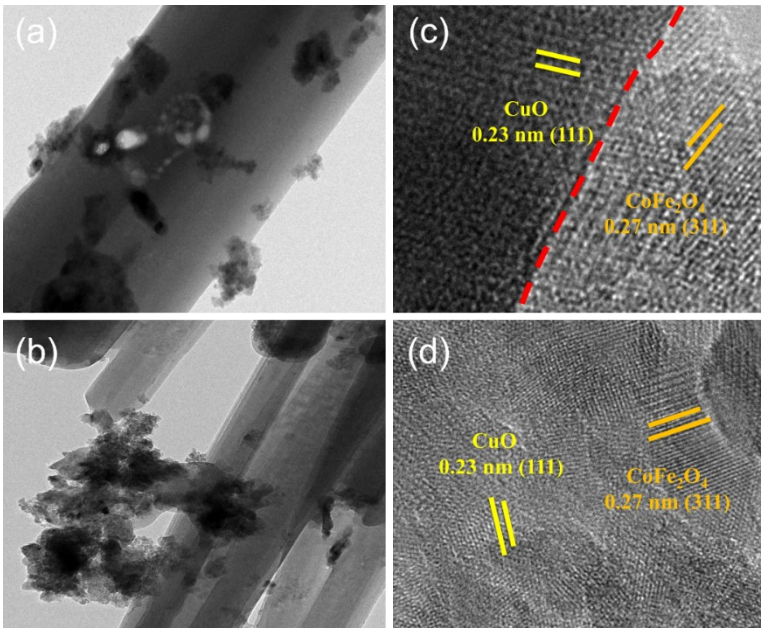

Fig. S21. The TEM images of catalyst (a) before and (b) after 50 h electrolysis at 300 mA cm^{-2}. The HRTEM images of catalyst (c) before and (d) after 50 h electrolysis at 300 mA cm^{-2}

Tab. S1 Comparison of performance of our catalyst with recently reported electrocatalysts.

Catalysts	Substrates	Voltage (V)	j (mA cm^{-2})	Con. (%)	Yield. (%)	FE (%)	Ref.
$CoFe_2O_4$@CuO/CF	1,2-Cyclohexanediol	1.50 1.70	115 170	93.8 92.4	79.5 /	88.9 84.0	*This Work*
2%Cu-$Ni(OH)_2$/NF	Cyclohexanol	/	100	/	84	55	*Angew. Chem. Int. Ed.* **2022**, 61 e202214977[1]
$CuCo_2O_4$/NF	Cyclohexanol	1.50	10	/	85	84	*J. Am. Chem. Soc.***2024**, 146, 1282[2]
CoMnOOH/NF	Cyclohexanol	1.45	10	100	64	/	*Angew. Chem. Int. Ed.* **2021**, 60, 8679[3]
NiOOH	Cyclohexanone	/	/	/	/	25	*Russ. Chem. Bull.* 2004, 53, 2310274[4]
NiV-LDH-NS	Cyclohexanone	1.76	170	/	/	83	*Nat. Comm.***2024** 15:7685[5]
Co_3O_4/GDY	Cyclohexanol	1.60	114	/	/	89	*Adv. Funct. Mater.* **2023**, 2310274[6]
$NiCo_2O_4/CeO_2$	Cyclohexanol	1.49	/	100	87	86	*Angew. Chem. Int. Ed.***2025**, 37, e202423432[7]
Mn−$Ni(OH)_2$/CP-1	KA oil	1.50	50	21.1	/	/	*ACS Sustainable Chem. Eng.***2024**, 12, 5907−5916[8]
$Cu_{0.81}Ni_{0.19}$/NF	KA oil	1.45	100	/	70	92	*J. Energy Chem.* 101 (**2025**) 7–15[9]

$Ni(OH)_2$-SDS/NF	Cyclohexanone	1.70	30	/	/	77	*Nat. Communications* (**2022**) 13:5009 [10]
$CuxNi_{1-x}(OH)_2$/CF	Cyclohexanone	1.57	7	/	/	71	*Exploration* **2024**,4:20230043. [11]
msig/ea-NiOOH-$Ni(OH)_2$/NF	Cyclohexanone	1.465	7	/	/	76	*J. Am. Chem. Soc.***2024**, 146, 1282-1293. [12]

Tab. S2 Summary of CHD oxidation under different applied potential using $CoFe_2O_4$@CuO/CF as electrocatalyst.

Electrocatalyst	Potential (V)	CHD Conversion (%)	Adipic acid selectivity (%)	Adipate Yield (%)	Faradaic efficiency (%)
$CoFe_2O_4$@CuO/CF	1.45	79.3	60.7	48.1	69.9
	1.50	93.8	84.8	79.5	88.9
	1.55	98.2	67.5	61.5	87.2
	1.60	94.1	63.2	59.5	86.1

Tab. S3 Summary of the CHD oxidation by CuO/CF, $CoFe_2O_4$/CF and $CoFe_2O_4$@CuO/CF at the same voltage.

Electrocatalyst	Potential (V)	CHD Converion (%)	Selectivity (%)			Adipate Yield (%)	Faradaic efficiency (%)
			Succinic acid	Glutaric acid	Adipic acid		
$CoFe_2O_4$@CuO/CF	1.50	93.8	0.06	15.1	84.8	79.5	88.9
$CoFe_2O_4$/CF	1.50	71	6.7	19.3	73.9	52.5	62.3
CuO/CF	1.50	66	9.8	24.9	64.8	42.8	55.5

Tab. S4 Comparisons of recent electrolysis performance of organic oxidation-coupled hydrogen production in two-electrodes electrolyzer.

Catalyzer	Substrates	Voltage (V)	J (mA cm^{-2})	FE (%)	Ref.
$CoFe_2O_4$@CuO/CF	1,2-Cyclohexanediol	1.12 1.60	10 300	85.7 82.3	This work
Ni_2P@$Ni1_2P_5$	Cyclohexanol	1.53	232	/	*Adv. Mater.* **2025**, *37*, 2502523[13]
$Co_2(OH)_3Cl$/FeOOH	Cyclohexanol	1.46	10	/	*CEJ. 442* (**2022**) 136264[14]
$NiCo_2O_4/CeO_2$	Cyclohexanol	2.00	200	75	*Angew. Chem. Int. Ed.* **2025**, *64*,e202423432[7]
Co_3O_4/GDY	Cyclohexanone	2.20	180	45	*Adv. Funct. Mater.* **2023**, 2310274[6]
$CuCo_2O_4$/NF	KA oil	3.00	200	52	*J. Am. Chem. Soc.* **146**, 15275–15285 (**2024**). [2]
$Cu_{0.81}Ni_{0.19}$/NF	KA oil	1.51	100	/	*J. Energy Chem.*101 (**2025**) 7–15[9]
$Ni(OH)_2$-SDS/NF	Cyclohexanone	1.90	28	20	*Nat. Communications* (**2022**) 13:5009 [10]
NiV-LDH-NS	Cyclohexanone	1.76	300	82	*Nat. Comm.***2024** 15:7685 [5]

-

Note 1. To evaluate the economic potential of a coupled electrolytic cell that simultaneously generates AA and H_2, the technoeconomic analysis (TEA) was carried out based on the modified model from prior reports.

The specific sample for the calculation of AA production under optimistic case assumptions:

Take the 1000 kg daily capacity of AA as an example at a current density of 0.3 A cm^{-2} with 86.0 % FE of AA at anode and 99.0 % of H_2 at cathode as an example:

1. The electricity price was considered to be 0.05 \$ kWh^{-1}.

2. The price of H_2O was 0.0007 \$ kg^{-1}. The price of H_2 was 2.5 \$ kg^{-1}. The price of O_2 was 0.108 \$ kg^{-1}. The price of CHD was 1.0 \$ kg^{-1}. The price of AA was 2.49 \$ kg^{-1} [1].

3. The operating voltage was set as 1.60 V.

Thus, the parameters needed in the cost calculation are determined as follows

The required **total current** is calculated as:

$$\textbf{Total Current} = \frac{1000\ \text{kg}}{\text{day}} \times \frac{\text{day}}{86400\ \text{s}} \times 1000\frac{\text{g}}{\text{kg}} \times \frac{\text{mol}}{146.14\text{g}} \times 6\text{e -} \times \frac{96485\ \text{C}/mol}{\text{mol}} \times \frac{1}{86.0\%} = 533 \quad (1)$$

Based on the operating voltage (1.6V), we can get the consumed **power** as follows:

$$\textbf{Power} = 1.60\text{V} \times 53312.59\ \text{A} \times \frac{\text{W}}{1000\ \text{kW}} = 85.30\ \text{kW} \quad (2)$$

By assuming the electricity price is 0.05 \$/kWh, the **electricity cost per ton of AA** is:

$$\textbf{Electricity cost per ton of AA} = 85.30\ \text{kW} \times 24\ \text{h} \times \frac{0.05\$}{\text{kWh}} = 102.36\ \$\ \text{ton - 1} \quad (3)$$

Material cost：

$$\textbf{Water} = 0.0007\frac{\$}{\text{kg}} \times \frac{18\ \text{g mol - 1}}{146.14\ \text{g mol - 1}} \times \frac{6\text{e -}}{2\text{e -}} \times \frac{99\%}{86.0\%} \times \frac{1000\ \text{kg}}{\text{ton}} = 0.29\ \$\ \text{ton - 1} \quad (4)$$

$$\textbf{1,2 - Cyclohexanediol} = 1.0\frac{\$}{\text{kg}} \times \frac{116.158\ \text{g mol - 1}}{146.14\ \text{g mol - 1}} \times \frac{1000\ \text{kg}}{\text{ton}} = 794.85\$\ \text{ton - 1} \quad (5)$$

The total cost

$$\textbf{The total cost} = 794.85\ \$\ \text{ton - 1} + 0.29\ \$\ \text{ton - 1} + 102.36\ \$\ \text{ton - 1} = 897.5\ \$\ \text{ton - 1} \quad (6)$$

The total revenue

$$\mathbf{AA} = 2.49\frac{\$}{\text{kg}} \times \frac{1000\ \text{kg}}{\text{ton}} = 2490\ \$\ \text{ton}^{-1} \quad (7)$$

$$\mathbf{H2} = 2.5\frac{\$}{\text{kg}} \times \frac{2\ \text{g mol}^{-1}}{146.14\ \text{g mol}^{-1}} \times \frac{6e^-}{2e^-} \times \frac{99\%}{86\%} \times \frac{1000\ \text{kg}}{\text{ton}} = 118.16\ \$\ \text{ton}^{-1} \quad (8)$$

The total revenue：

$$\textbf{The total revenue} = 2490\ \$\ \text{ton}^{-1} + 118.16\ \$\ \text{ton}^{-1} = 2608.16\ \$\ \text{ton}^{-1} \quad (9)$$

The total income：

$$\textbf{The total income} = 2608.16\ \$\ \text{ton}^{-1} - 897.5\ \$\ \text{ton}^{-1} = 1710.66\ \$\ \text{ton}^{-1} \quad (10)$$

Compare the economic benefits of two production processes, traditional electrolysis of water and daily production of 1000 kg of AA, under the same energy consumption. The operating voltage was set as 1.23 V

Total electrical energy

$$ETotal\ electrical\ energy = 85.30\ \text{kW} \times 24\ \text{h} = 2047\ kWh \quad (11)$$

$$Eelectrical\ energy = 2047\ kWh = 7.3692 \times 109\ J \quad (12)$$

Total charge:

$$\mathbf{Q} = \frac{\text{E}}{\text{U}} = \frac{7.3692 \times 109\ J}{1.23\text{V}} = 5.991 \times 109\ C \quad (13)$$

Faraday's laws:

$$Q = n \times F$$

$$ne = \frac{5.991 \times 109\ C}{96485\ C/mol} = 6.209 \times 104\ mol \quad (14)$$

Hydrogen quality:

$$nH2 = \frac{6.209 \times 104}{2} = 3.1045 \times 104\ mol \quad (15)$$

$$MH2 = 3.1045 \times 104\ mol \times 2\ g/mol = 6.21 \times 104\ g \quad (16)$$

Oxygen quality:

$$nO2 = \frac{3.1045 \times 104}{2} = 1.552 \times 104\ mol \quad (17)$$

$$MO2 = 1.552 \times 104\ mol \times 32\ g/mol = 4.97 \times 105\ g \quad (18)$$

Material cost：

$$\mathbf{nH2O} = \mathrm{nH2} = 3.1045 \times 104\ mol$$

$$\mathbf{mH2O} = \mathrm{n}H2O \times 18g/mol = 3.1045 \times 104\ mol \times 18\ g/mol = 558.81k$$

)

$$\mathbf{Water} = 0.0007\frac{\$}{\mathrm{kg}} \times 558.81kg = 0.391\$\ \mathrm{ton}-1 \quad (21)$$

The total revenue

$$\mathbf{H2} = 2.5\frac{\$}{\mathrm{kg}} \times 62.1kg = 155.25\ \$\ \mathrm{ton}-1 \quad (22)$$

$$O\mathbf{2} = 0.108\frac{\$}{\mathrm{kg}} \times 497kg = 53.68\ \$\ \mathrm{ton}-1 \quad (23)$$

The total revenue = 155.25 $ ton - 1 + 53.68 $ ton - 1 = 208.93 $ ton - 1 (24)

The total income：

The total income
= 208.93 $ ton - 1 - 0.391 $ ton - 1 = 208.539 $ ton - 1
(25)

Economic Benefit Comparison:

Comparison = 1813.02 $ ton - 1 ÷ 208.539 $ ton - 1 = 8.7 (26)

References:

[1] X. Liu, Y.-Q. Zhu, J. Li, Y. Wang, Q. Shi, A.-Z. Li, K. Ji, X. Wang, X. Zhao, J. Zheng, H. Duan, Electrosynthesis of adipic acid with high faradaic efficiency within a wide potential window, Nature Communications 15(1) (2024).